JOURNAL OF MATERIALS SCIENCE **40** (2005) 6169–6173

Chromaticity, brightness and aging of silica spray coated zinc sulfide silver phosphor particles

G. VILLALOBOS*, J. SANGHERA
U.S. Naval Research Laboratory, Washington, DC 20375

R. MIKLOS
SFA Inc., Largo, MD 20774

F. KUNG
University Research Foundation, Greenbelt, MD 20770

S. BAYYA, I. AGGARWAL
U.S. Naval Research Laboratory, Washington, DC 20375

Published online: 8 September 2005

A spray drying approach was used to coat 15 nm SiO_2 continuous films onto ZnS:Ag phosphor particles. The coating was deposited on the particles by simultaneously spraying a slurry consisting of a solution of TEOS and ethanol with the solid phosphor particles into a heated drying column. The cathodoluminescent spectra of silica coated phosphor has CIE 1931 chromaticity coordinates of $X \sim 0.055$, $Y \sim 0.085$, brightness that is 90% of the uncoated phosphor brightness, and improved aging behavior under laboratory testing conditions.

1. Introduction

The high efficiency phosphors developed for field emission displays (FED), plasma displays, and white LED's tend to be degraded by the operating environment and/or the devices' manufacturing conditions [1–4]. Buffer coatings have been studied as a method to isolate the phosphor from harmful species. However, coatings are difficult to deposit continuously, hermetically, and thin enough so the phosphor brightness is not severely degraded [5–7].

We have demonstrated the use of simultaneous spraying of particles and coating precursors to successfully deposit 15 nm continuous films on 5 μm sized zinc sulfide: silver phosphor particles [8]. In this paper we will expand on the deposition process and present the results of photoluminescent (PL), cathodoluminescent (CL) efficiency, and cathodoluminescent aging behavior of the SiO_2 coated phosphor as measured in laboratory settings. Aging tests have shown a dramatic improvement in behavior between the coated and un-coated phosphors, while phosphor efficiency and chromaticity (both CL and PL) are within 10% of uncoated values. Future work will include testing the coated phosphor in LED's, investigation of other coating materials, and coating phosphor materials for use in plasma devices.

2. Experimental

A silica coating solution based on a standard dip coating formula was used. TEOS (Fisher Scientific) was mixed in a 1:1 ratio with ethyl alcohol (200 proof). The catalyst was 0.15% by volume HCl (12 M Fisher reagent grade), and the solution was pre-hydrolyzed with one equivalent of de-ionized water. The resulting stock solution was stored in a freezer and used as needed. Storing did not degrade the solution; stock solutions over two years old were successfully used.

Immediately prior to spraying, the phosphor to be coated was suspended in 200-proof ethyl alcohol and the stock solution added. The amount of stock solution was dependent on the desired thickness of the coating, thicker coatings merely requiring more stock solution. The ZnS:Ag phosphor particles used are manufactured by Nichia and are listed as 2–8 μm particle size distribution with an average of 5 μm. These phosphor particles were specifically ordered without the nano-sized silica particulate that Nichia deposits on phosphor surfaces to improve rheological characteristics. The nano silica particles tended to create tears in the coating. The particle morphology was further characterized using SEM (Leo 1550 Scanning Electron Microscope, LEO Electron Microscopy Inc., Thorwood, NY).

*Author to whom all correspondence should be addressed.
0022-2461
DOI: 10.1007/s10853-005-3162-6

The spraying system was built in-house and consists of a spray head, two 1.3 m long by 0.23 m diameter silica tubes stacked one on top of the other to create an 2.6 m drying column that could be heated to 500°C, and a cyclone separator to remove the coated particles from the gas stream. The drying column had three independently controlled external resistance heaters to allow the formation of a temperature graded drying zone. The heating zones were adjusted to prevent complete drying of the particle/drop until it had dropped halfway through the drying column. Inserting SEM stubs at various heights along the column and examining the adhered particles in the SEM was used to determine the degree of drying. The following temperature gradient was found to work best: the top of the 2.6 m long column was at room temperature, the top heater was placed 30 cm from the top and held at 150°C, the middle heater was 10 cm below the place were the two tubes were joined and held at 270°C, while the bottom heater was at approximately 300°C. Air could be admitted immediately before the cyclone to reduce the temperature in the cyclone. An exhaust fan attached to the outlet of the cyclone supplied suction to overcome the chimney effect in the drying column. The precursor suspension was sprayed without allowing gelation to occur in the container. Gelation occurred while the slurry drops were falling through the drying column.

Simultaneous DTA/TGA (SDT 2960, TA Instruments, New Castle, DE) was used to determine the temperatures for organic burn out and treating of the coated particles. In general, the coated phosphor was heat treated at 280°C for 2 h in air to remove residual organics from the coating solution and at 650°C in argon to further densify the coating. Temperatures above 650°C tended to degrade the phosphor brightness. The physical effect of the heat treatment was determined by observation of the coating on the LEO SEM and by an HCl (Fisher Scientific 12 molar reagent grade acid) acid test. The HCl acid test consists of placing 0.1 g of phosphors in the bottom of a crystallizing dish and filling with 25 ml of reagent grade acid. Uncoated ZnS phosphor particles are readily soluble in HCl, whereas the coating should protect the phosphor from dissolution.

The photo (PL) and cathodoluminescent (CL) chromaticity and brightness were measured using, respectively a Fluorometer (Spex Fluoromax, Edison, NJ) and a Spectrophotometer (SpectraScan 705, PhotoResearch, Chatsworth, CA). An SEM (Amray 1700, Bedford, MA) was used as the electron source for the CL measurements. PL emission was excited using a 275 nm wavelength, while CL was performed with a 5 keV electron beam. Aging tests were conducted at Sandia National Labs using a continuous e-beam operating at 3 kV and 61 mA/cm^2. This resulted in an electron dose of 0.22 C/cm^2/h. In all cases the phosphors were measured using a deep powder patch.

3. Results and discussion

For this particular spray coating procedure to work it is important that no gelation or precipitation of the coating precursors occurs before the particles and precursor solution are sprayed into the thermally graded hot zone. In its idealized form, each phosphor particle is sprayed out in its own individual droplet of precursor solution. Precipitation/gelation of the precursor occurs while the solvent evaporates as the particle/droplet combination falls through the hot zone. If a precipitate forms on the particle or in solution prior to spraying the particles will have a lumpy appearance. The precipitates also tend to cause tears and flaws in the coating and are therefore prevented from forming. If there is more than one particle per spray drop, they will agglomerate.

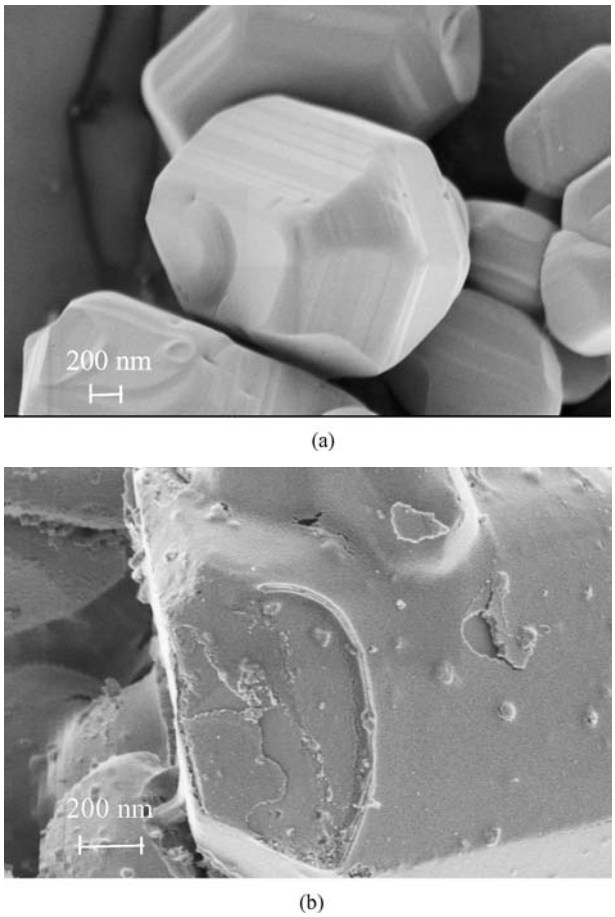

Figure 1 (a) Properly coated ZnS phosphor showing a smooth, continuous SiO_2 and (b) Unoptimized SiO_2 coated ZnS phosphor showing tears and holes.

Well-coated particles show little visual evidence of being coated. A good coating is adherent and conforms to the shape of the phosphor particle. Fig. 1a is a micrograph at 10,000*X* magnification of SiO_2 coated particles with a uniform and continuous coating. From the HCl test results, explained below, it appears that more than 90% of the phosphor particles are properly coated. Fig. 1b is an SEM micrograph at 20,000*X* magnification showing an earlier un-optimized SiO_2 coating on a phosphor particle. The un-optimized coating is useful in showing that a coating is present while the edges of the large tears can be used to measure the coating thickness and confirm the calculations used to determine particle to precursor weight and dilution ratios. A way to test the integrity of the SiO_2 coating is to immerse the particles in 12 M HCl. Fig. 2 is a coated particle that was immersed in concentrated HCl. Since

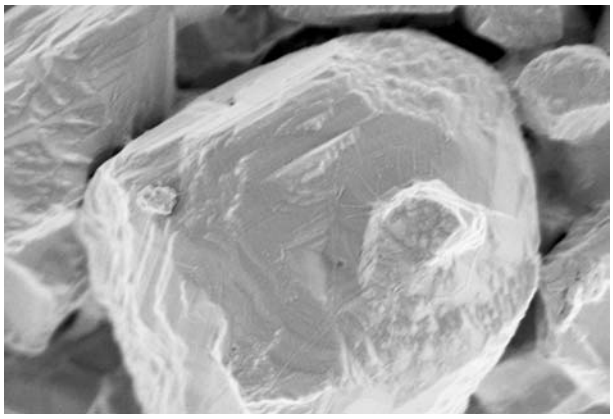

Figure 2 SiO_2 coated particles after overnight soak in HCl acid.

HCl readily dissolves ZnS, uncoated particles dissolve on contact with the acid. The coated phosphor particle in Fig. 2 has survived an overnight stay in the acid. However, the roughened surface of the particle is evidence of acid penetrating the coating. It is also interesting to note that the coating continues to conform to the underlying surface. This effect of a collapsing oxide coating has also been noted on thin aluminum oxide films [9]. The acid penetration appears to be through nano pores present in some areas of the coating. Fig. 3 is a 250 volt high resolution SEM micrograph highlighting porosity on one surface, note that the other particle surfaces visible on the micrograph contain significantly fewer pores. Since the porosity appears to be non-uniform and localized to certain surfaces, the HCl attack rate is considerably slower as compared to an uncoated phosphor or one with an un-optimized coating containing tears. There was less than a 10% drop in the weight of the phosphor powder after soaking in the acid overnight.

The spraying coating parameters can be separated into those that control the coating characteristics and those that control particle agglomeration. The coating morphology and adherence is mainly related to the temperature gradient in the drying column, while agglomeration depends mainly on the particle to liquid ratio.

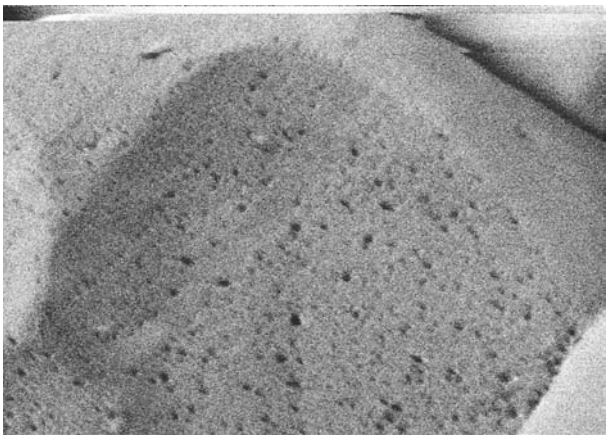

Figure 3 Coated surface exhibiting nano porosity on one surface and very little porosity on the other surfaces.

A standard SiO_2 dip coating formula was found to work well for spray coating. It was chosen for spraying because the drying dynamics of the sprayed particles are similar to those in dip coating. In both spray and dip coating, the evaporation of solvent aids precipitation/gelation. As the solvent evaporates, the concentration of the sol increases thereby increasing the viscosity until precipitation or gelation (depending on the precursors used) occurs [10, 11].

3.1. Column temperature gradient

A vertical temperature gradient in the spray column controlled the evaporation rate of the drop. Spraying into a hot chamber, as is normally done when using a conventional spray drier, resulted in partial coatings and delamination at the coating phosphor interface because the high initial evaporation rate caused the formation of a crust around the still liquid interior [5, 11, 12]. Further heating, evaporation, and gelation of the interior material causes the outside shell to collapse resulting in irregular coatings and pieces of broken shells. The three independent heaters on the drying column allowed the temperature gradient to be tailored so as to allow slow initial evaporation, gelation, and finally to partially sinter the coating before reaching the cyclone. Room temperature air could be admitted to the cyclone to reduce the temperature to approximately 150°C. This prevented baking the particles onto the cyclone walls.

3.2. Agglomeration

The dilution of the spray suspension was chosen to minimize the size of the agglomerates based on the average particle and droplet diameters. Agglomeration is prevented by not spraying multiple particles per spray drop. If there is more than one particle in a drop, they will be stuck together by the coating. Single particle per drop spraying would be simplified by having an atomizer that produces a consistently tight size distribution of drops, in addition to having a phosphor with a mono-dispersed particle size. Unfortunately neither is available.

SEM examination showed that the average particle size was in the 2–5 μm range. Fig. 4 shows curves from a simple geometric calculation relating the particle diameter to the number of particles per drop and the dilution ratio for an atomizer producing on average 45 μm drops. The curves suggest that the 1:0.6 dilution (1 g of phosphor to 0.6 liters of solvent) would tend to put one 3 μm particle per spray droplet while the 1:1.2 and 1:1.8 dilutions would put roughly one 2 μm particle per drop. Experimentally, the 1:0.6 and 1:1.2 dilutions tended to form agglomerates while the 1:1.8 dilution did not. Dilutions higher than 1:1.8 did not appear to have any advantage in decreasing the number of agglomerates, but did result in the formation of silica spheres that did not contain phosphor particles. The major impact on agglomerate formation was from the sub-micron to 2 μm particles. These particles tended to segregate and form large spherical agglomerates at the lower dilutions as is shown in Fig. 5.

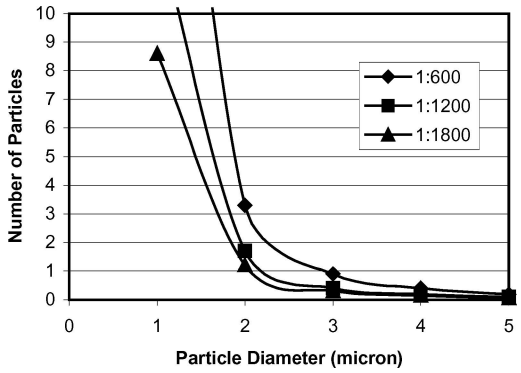

Figure 4 Dilution curves for a 40 μm droplet size.

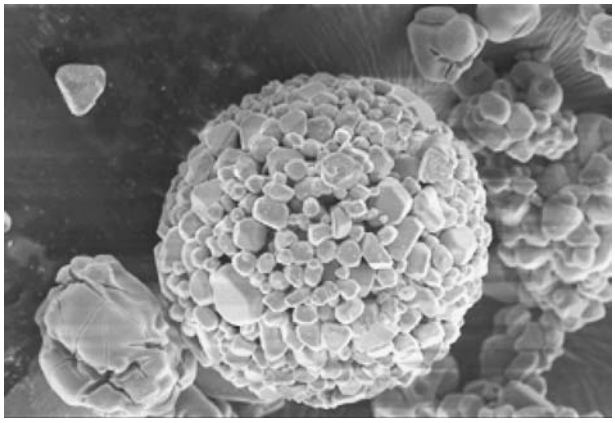

Figure 5 Large agglomerates formed using low dilutions.

3.3. Luminescence

Fig. 6 shows the cathodoluminescent spectra of phosphors: with no coating (un-coated), with one of our optimized coatings (new coating), and with an early, un-optimized coating (old coating). The shape of the cathodoluminescent emission curves of the uncoated phosphor and a phosphor with a new coating are very similar with the coated phosphor having about 90% of the brightness of the uncoated phosphor. The spectrum of the phosphor with an old coating (before we had optimized the process) has much lower brightness and its emission tails off into the green wavelengths instead of returning to zero.

The coated phosphors have been heat treated to remove residual organics and to densify the coating. The spectra of coated phosphor that have not been heat-treated show very little degradation. After heat-treating, the spectra of uncoated phosphors (used as control samples) are not changed, the phosphors with the optimized coatings show a decrease of about 10% brightness as shown in Fig. 6, and the phosphors with the old coatings show considerable degradation and the formation of a large green tail. It is apparent that unwanted reactions are occurring during the heat treatment operation.

The size of the green tail can be enhanced when the heat treating times are lengthened or the phosphor is immersed in water prior to heat treatment. If the coated phosphor is placed in a breaker of water and heat treated, the tail almost becomes a separate peak with a maximum at approximately 525 nm. Unfortunately, even samples with very large green components do not show the presence of a different phase using XRD making it difficult to determine the degradation mechanism. The older coatings had greater amounts of water added to prehydrolyze the TEOS than the newer coatings. It may be that the extra water used increased the amount of degradation.

In order to test whether formation of ZnO caused the green tail, un-coated ZnS phosphor particles were heat treated in air and oxygen for various times and temperatures. The brightness tended to be severely decreased, but the green tail did not form. XRD of the more aggressively oxidized samples showed a complete conversion to ZnO while the less aggressive treatments showed various ratios of ZnS to ZnO.

Photoluminescent spectra were also taken, but are not reported here. The photoluminescent spectra are similar to the cathodoluminescent spectra when a 275 nm excitation source is used. As the wavelength of the photoluminescent excitation is increased the green tail is reduced until it disappears when the excitation wavelength reaches the 330–350 nm range. However, the brightness of the phosphors does not change as the excitation wavelength is increased. Fig. 7 shows the CIE 1931 chromaticity chart and marks on the coordinates of the coated and uncoated phosphors when using CL excitation. Note that there is a only a slight green shift in the coordinates of the well-coated phosphors while the older phosphors are severely shifted.

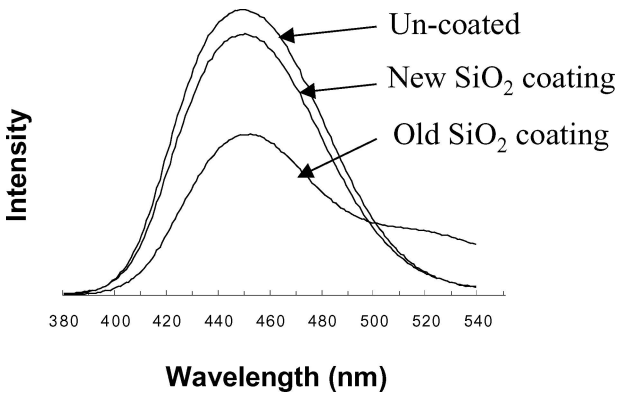

Figure 6 Cathodoluminescent spectra.

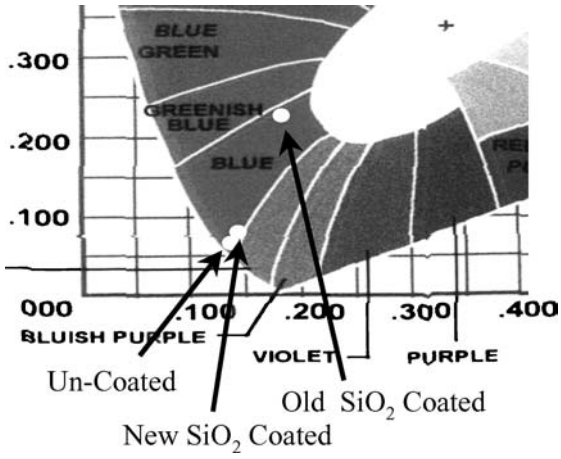

Figure 7 CIE 1931 coordinates.

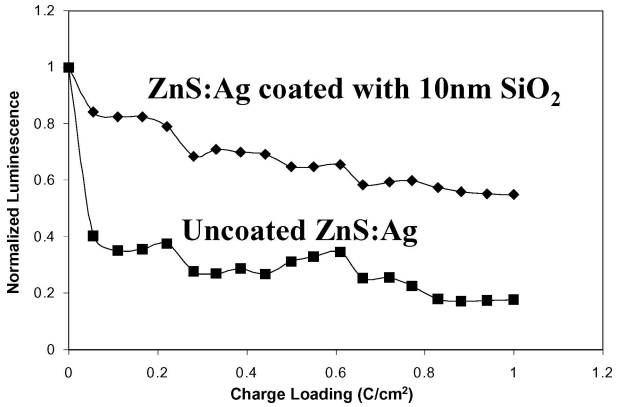

Figure 8 Phosphor aging results.

3.4. Aging

Accelerated aging shows that the coated phosphor has a slower initial degradation than the un-coated phosphor, Fig. 8. The slope after the initial degradation is slightly shallower for the coated phosphor. The end result is that the coated phosphor retained 60% of its initial brightness, while the un-coated only had about 20% of its initial brightness at the end of the test. There is no explanation for the difference in the initial degradation, although it has been seen in materials coated with TaSi(13). The secondary degradation could be related to the nano-porosity in the coating. The residual atmospheric species in the vacuum could penetrate through the pores and attack the phosphor surface. This effect could be similar to that of the acid penetrating the coating during the overnight soak.

4. Conclusion

We were able to uniformly coat micron sized phosphor particles with nanometer thick SiO_2 using a spray drying procedure. The coatings were continuous and able to protect the phosphor from degradation when submerged in reagent strength HCl acid. The resulting chromaticity coordinates were within 10% of the values for uncoated samples while the ageing characteristics were greatly improved. This procedure should be applicable to the newer high efficiency phosphors that are difficult to use and process due to their reactivity and general lack of stability. The coating serves to isolate the phosphor from the environment and could therefore be used to protect both the phosphor and the device.

References

1. R. PETERSON, *Inform. Disp.* **3** (1997) 22.
2. H. YAMAMOTO, *J. Soc. Inform. Disp.* **4** (1996) 165.
3. H. BECHTEL, W. CZARNOJAN, M. HAASE, W. MAYR and H. NIKOL, *Phillips J. Res.* **50** (1996) 433.
4. B. K. WAGNER, J. PENCZEK, S. YANG, C. STOFFERS and C. J. SUMMERS, Proceedings 1997 International Display Research Conference (1997) p. 330.
5. J. H. JEAN and S. M. YANG, *J. Amer. Ceram. Soc.* **83** (2000) 1928.
6. Y. AZUMA, K. NOGAMI and N. OHSHIMA, *J. Ceram. Soc. Jpn.* **100** (1992) 646.
7. L. NIKOLIC and L. RADONJIC, *Ceram. Intl.* **24** (1998) 547.
8. G. VILLALOBOS, *et.al. J. Amer. Ceram. Soc.*, **85** (2002) 2128.
9. K. V. LOGAN, J. T. SPARROW and W. J. S. MCLEMORE, in "Combustion and Plasma Synthesis of High Temperature Materials", VCH (Verlag Chemie, 1990) p. 219.
10. C. J. BRINKER and G. W. SCHERER, in "Sol-Gel Science", (Academic Press, 1990).
11. K. MASTERS, in "Spray Drying Handbook", (John Wiley & Sons, 1985).
12. G. L. MESSING, S. C. ZHANG and G. V. JAYANTHI, *J. Amer. Ceram. Soc.* **76** (1993) 2707.
13. J. M. FITZ-GERALD, T. A. TROTTIER, R. K. SINGH and P. H. HOLLOWAY, *Appl. Phys. Lett.* **72** (1998) 1838.

Received 4 May 2004
and accepted 13 April 2005